pp 2001–2018.
doi:10.1017/aer.2020.64

Combustor-inlet interactions in a low-order dynamic model of ramjet engines

K. Liu
Shenzhen Graduate School
Harbin Institute of Technology
Shenzhen 518055
China

T. Cui
taocui@zju.edu.cn
School of Aeronautics and Astronautics
Zhejiang University
Hangzhou 310027
China

ABSTRACT

The coexistence of multiple stable states is indicative of self-organising processes occurring in the course of the combustor-inlet interactions in a ramjet engine and give rise to the appearance of various nonlinear phenomena. This paper provides a dynamic model that can describe the multiple stable states and the corresponding nonlinear effects to further investigate the dynamic interactions between combustor and inlet in a ramjet engine. Our study shows the whole engine can display distinct dynamic behaviours ranging from irreversibility to hysteresis and to various mode transitions, depending on different physical parameters. With the model, we also illustrate the role of the instability of the normal shock wave in impacting the whole engine's nonlinear dynamics. Additionally, we extend the previous studies of the classification of combustor-inlet interactions from a static framework to a dynamic framework, which helps to clarify the transient processes of the nonlinear interactions. This work offers a quantitative illustration of the combustor-inlet interactions in a ramjet engine by revealing its nonlinear dynamics and associated characteristics, therefore advancing our understanding of the nonlinear phenomena that exhibit in ramjet engines.

Keywords: Ramjet engine; Dynamic model; hysteresis

NOMENCLATURE

a sound speed, m/s
A cross-sectional area, m^2

Received 22 February 2020; revised 30 June 2020; accepted 1 July 2020.

k ratio of specific heats
M Mach number
p static pressure, Pa
P total pressure, Pa
q mass flow function
R gas constant, J/Kg/K
T static temperature, K
T_t total temperature, K
x position of shock wave, m
$\dot{m}$ mass flow rate, Kg/s
θ empirical constant
ρ density
τ heat addition ratio
σ forward propagation time constant, s
Φ defined by Eq. (6)
Ω amplitude variation induced by heat addition

Superscripts

∞ incoming flow
0 inlet entrance
m first throat
1 before the shock wave
2 after the shock wave
3 combustor entrance
4 combustor exit
s shock wave
th second throat

Subscripts

$\_$ steady-state parameter
$\sim$ nondimensionalised parameter

1.0 INTRODUCTION

Combustor-inlet interaction is a longstanding classic problem in air-breathing propulsion engineering that is still not fully understood. Indeed, the suppression of combustor-inlet interactions associated with heat release, which can cause unfavourable inlet unstart events, represents a technological advancement of critical importance. Inlet unstart can cause violent and unsteady thermal and aerodynamic loads, even leading to the destruction of the engine, evidenced by the recent failure of the second X-51 flight experiment. The causes of inlet unstart can be broadly divided into two groups: aerodynamic phenomena associated with the

https://doi.org/10.1017/aer.2020.64 Published online by Cambridge University Press

inlet flow itself, such as changes in Mach number, angle-of-attack, or boundary layer separation on an intake surface, and processes that originate downstream in the combustion chamber of the engine.[1–3] The latter, involving complex interactions between the combustor and inlet, are more difficult to understand and form the focus of the present investigation. Combustor-inlet interactions in ramjet/scramjet engines are directly associated with critical operational processes such as combustion mode (ramjet/scramjet mode) transition and the onset of inlet unstart. Over the past few decades, much work has been accomplished toward understanding the mechanism of combustion mode transition.[4] For example, Sullins[5] experimentally demonstrated the mode transition in a ramjet combustor and observed the instability of the shock system during the transition. Chun[6] observed that the flame was located far downstream of the injector with low equivalence ratio; as the fuel amount increased, the flame jumped from far downstream to the end of the injector and mode transition occurred. The transition was caused by the change in shock wave structure triggered by the pressure rise due to strong combustion. Eggers[7] discovered that under certain conditions, small deviations in fuel flow may significantly affect the movement of shock trains, and the operation mode may shift from scramjet mode to ramjet mode. Goyne[8] investigated the transition between supersonic and subsonic combustion in a hydrogen-air combustor. Riggins[9] conducted a numerical study and reported that the transition behaviour is characterised by a decrease in entropy (increase in total pressure) with an increment of heat release. In addition to these studies on combustion mode transition, much work has also been done on the mechanism of combustion-related inlet unstart. An incipient unstart is typically brought about through one of two processes, or a combination thereof: (1) excessive heat release in the combustion chamber, leading to the flow reaching sonic conditions and thus becoming thermally choked; (2) the combustion-induced adverse pressure gradient causing the wall boundary layer to separate, resulting in the formation of shock waves, which then propagate upstream.[10] If the combustion-related pressure rise is too great, the shock waves will continue moving upstream and unstart the inlet. The flow phenomena associated with the onset of unstart have been the subject of many numerical and experimental investigations. Ferri[11] presented early approaches to a closely integrated inlet–combustor design. He created concepts that tailored the aerothermodynamics of fuel injection, mixing, and combustion to the desired engineering features of the engine. In the ground-test programs to develop the techniques, considerable problems and delays were encountered due to combustor–inlet interactions. Billig and Dugger[12] presented methods of modelling the process for cycle performance calculations and there were many subsequent studies correlating the strength of the pre-combustion shock with heat release, and others on the length of isolator needed to prevent propagation of the disturbance up to the inlet. E T Curran et al.[13] used the "H-K" (thermal energy versus kinetic energy) coordinates to explore and analyse the complex interactions between the combustor and inlet. They concluded that the nature of interaction between the combustor and inlet is different for ramjet and scramjet operations. Shimura et al.[14] carried out experiments on a large-scale scramjet engine. As the equivalence ratio was increased, pressure spikes were observed to develop with a frequency that increased with the strength of the subsequent unstart. The formation of an upstream-propagating separation bubble was postulated as the source of the pressure spikes. O'Byrne et al.[15] investigated thermal choking behaviour in a simple combustor in the T_3 reflected-shock wind tunnel. The experiments were performed to examine the nature of the processes that lead to unstart in a thermally choked combusting environment at different combustor entrance Mach numbers and fuel-air equivalence ratios. Some evidences that combustion had an effect on the propagation of the

https://doi.org/10.1017/aer.2020.64 Published online by Cambridge University Press

shockwave, in particular at the lower Mach number condition, were provided by the shadowgraph images and the pressure measurements. In addition, many other experiments and numerical investigations were performed to examine the effect of varying inlet Mach number and fuel-air equivalence ratio on the nature and extent of the interaction between the combustor and inlet.[16–18] Some mechanisms that might contribute to this phenomenon were presented. These included separation of the boundary layer in the duct, formation of a detonation, and formation of shock waves by the region of thermally choked flow, and et al. In some cases, the combustion-induced pressure rise was replaced with mechanical throttling of the flow. Chen et al., Bogar et al., and Sajben et al.[19–23] conducted a series of experimental investigations into inlet flows to better understand the flow behaviour in a ramjet engine. Various flow phenomena, such as shock, induced separated flows, and shock/acoustic wave interactions were investigated in detail. Van et al.[24] studied a small-scale rectangular inlet at Mach 3. Cowl length and cowl height parameters were studied for their effect on the inlet starting characteristics, and inlet unstarts were classified as "hard" or "soft." Hard unstarts occurred when the flow choked at the inlet throat whereas soft unstarts occurred as large-scale separation developed within the inlet. For shorter cowls and higher cowl heights, hard unstarts were prevalent whereas the softer unstarts occurred for the longer cowl lengths and lower cowl heights. Various flow characteristics were observed and measured by applying simultaneous high-speed schlieren imaging and surface pressure measurements. Cui et al.[25] developed a low-order model of the time-dependent behaviours of shock motion to describe the bistability and hysteresis behaviours of shock motion in a supersonic inlet. Theoretical studies were also carried out focusing mostly in transient regimes and ramjet combustor-inlet interactions. These analyses mostly assumed simple geometries, inviscid flows, while the solution methods involved asymptotic methods, and (or) linear stability analysis. Culick and Rogers[26] analysed the stability of normal shocks in the diverging section of inlets for ramjet engines. It was determined that stability of the normal shocks in diverging channels could be unfavourably influenced by the separation region created downstream of the shock. Hsieh and Yang[27] investigated the flow structures in a supersonic ramjet engine by considering both the internal flowfield in a mixed compression inlet and a coaxial dump combustor. Their calculations suggested a strong coupling between the combustor and inlet. At present, the problem of combustor-inlet interactions remains confusing to some degree. There are still questions concerning the complex multiple interactions of shock waves with the boundary layer, coupled heat release/shock wave generations and thermal chocking effects. Despite the body of existing work, theoretical and experimental efforts aimed at describing the physics of combustor-inlet interactions are an ongoing endeavour.

Previously we applied topological theory to analyse the physics of combustor-inlet interactions in a ramjet engine, and concluded that the complex combustor-inlet interactions are governed by a geometrical rule.[28] Further, we made a further step to use the concept of classification to mathematically rationalise the complexity of combustor-inlet interactions. As a result, we proved analytically that there are mathematically 72 types of combustor-inlet interactions in a ramjet engine, 11 of which are physically existent.[29] All these studies, however, were performed in static frameworks, and can only make direct, instantaneous link between system states and external perturbations using algebraic relationships. The disadvantage of the static analysis lies in its disability in describing the time-dependent changes in the state of ramjet engine, and accordingly the main obstacle is that the algebraic equations cannot account for the dominate dynamic processes of the system, such as the unstable positive-feedback effect and the duct volume effect. These effects are inherited in the system and have strong influence on the complex combustor-inlet interactions in ramjet engine. For example,

https://doi.org/10.1017/aer.2020.64 Published online by Cambridge University Press

it is the existence of unstable positive-feedback effect that introduces such nonlinear effects as multistability and hysteresis to ramjet engine, which will further give rise to the occurrence of complex combustor-inlet interactions.

Good models are simple, yet capture the essentials. The present study is undertaken to provide a new low-order dynamic model for capturing the nonlinear properties inherited in ramjet engines. The merit of the model is that it can describe the multistability phenomena of ramjet engines as well as the diverse hysteresis behaviours in the transitions among the engine's multiple states, which can be used as a theoretical basis to dynamic analysing the complex interactions in ground and flight experiments. Additionally, we extend the previous studies of the classification of combustor-inlet interactions from a static framework to a dynamic framework, which helps to clarify the transient processes of the nonlinear interactions. Finally, this model, consisting of a set of nonlinear, first-order differential equations, allows for rapid calculations of system's dynamics and can be a starting point towards a control-oriental dynamic model of ramjet engine.

2.0 LOW-ORDER DYNAMIC MODEL

The coexistence of multiple stable steady states, referred to as multistability, is generally associated with a phenomenon of hysteresis in which a system jumps back and forth between the two branches of stable states for different critical values of some control parameter. Multistability and hysteresis are indicative of self-organizing processes occurring in the course of the combustor-inlet interactions and give rise to the appearance of various combustor-inlet interactions in ramjet engine. The present study intends to provide a dynamic model, which can describe these nonlinear effects to further investigate the dynamic interactions between combustor and inlet. The complexity of dynamical behaviours involving multistability and hysteresis originates from the memory effect of initial states and the existence of multi-solution domain. The control of these systems thus depends not only on the instantaneous value of the input but also on the history of its operation. A better mathematical description of these nonlinear effects may be useful as a guide in thinking about the stability mechanism, designing the control routes, and actively controlling the dynamic behaviours of combustor-inlet interactions in ramjet engine.

The analytical dynamic model used is constructed with assumptions similar to those in the Kantrowitz theory: (1) ideal gas and inviscid flow; (2) upstream conditions are constant; (3) a fully enclosed inlet, i.e., the freestream velocity is normal to the entry plane, as shown in Fig. 1; (4) the influence of the oblique shock waves on the system's dynamics is not considered. These assumptions make a drop in model accuracy, but enable an analytical investigation, and similar assumptions have been made by many other authors.[26,30–34] Under the preceding assumptions, a ramjet engine has three operation modes, i.e., scramjet mode (*S*), ramjet mode (*R*), and inlet unstart (*U*) as shown in Fig. 2. Generally, the normal operation mode of a ramjet engine is "ramjet mode," and the thermal choking mechanism in supersonic flow gives rise to the appearance of normal shock wave at the diverging channel of the inlet (see Fig. 2(a)). Under critical conditions, the increase of heat addition or the decrease of inflow Mach number will cause the shock wave to move upstream and result in "inlet unstart" (see Fig. 2(b)). Once the heat addition of the combustor is not enough to maintain the choking conditions at the nozzle throat, the normal shock wave will move toward the nozzle throat and finally disappear. As a result, the combustor flow will be supersonic, and we define this operation state as "scramjet mode" (see Fig. 2(c)). If one or more of the control parameters, such as

https://doi.org/10.1017/aer.2020.64 Published online by Cambridge University Press

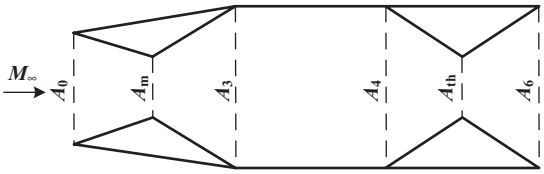

Figure 1. Schematic diagram of a ramjet engine.

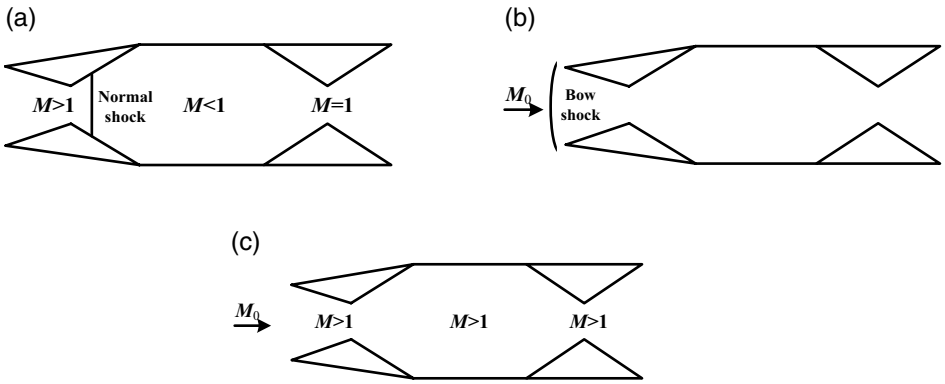

Figure 2. Operation modes of a ramjet engine. a) Ramjet mode (*R*), b) Inlet unstart (*U*), c) Scramjet mode (*S*).

τ, A_m, A_3, A_5, or M_∞, are altered to critical values, switches between these operation modes will take place. For the present investigation, the influence of the oblique shock waves on the system's dynamics is not considered. When the engine operates in the "inlet unstart" mode, there will be no oblique shock waves in the channel flow. When the engine operates in the ramjet or scramjet mode, there will be an oblique shock wave at the inlet entrance. In the ramjet mode, the neglect of the oblique shock wave will cause a deviation of the calculated position of the normal shock wave, because the total pressure loss of the oblique shock wave is incorporated into the normal shock wave. As a result, the calculated total pressure loss of the normal shock wave will be slightly larger, and the position of the normal shock wave will get closer to the inlet throat. In the scramjet mode, the neglect of the oblique shock wave will cause a deviation of the calculated Mach number of the channel flow as well as pressure and temperature. The neglect of the oblique shock wave will introduce the corresponding model error, but it has no influence on the description of the engine's qualitative nonlinear behaviours. At the same time, the characteristic time of the motion of the oblique shock wave is small enough to be neglected and has little influence on the whole system's dynamics.

The strong interactions between combustor and inlet are mainly determined by the stability of shock motion in ramjet engine. The shock wave responds to both upstream and downstream perturbations. Under the preceding assumptions, consideration is now limited to downstream perturbations that arise from the choking flow at the throttle throat. During any transient operation, the shock wave and the choking flow at the throttle throat interact with each other, and the inlet flow dynamics is mainly determined by these two transient processes as well as the perturbation propagations between them. The shock dynamics itself can be thought as wave propagation dependent on the velocity of the shock wave. The choking dynamics is mainly

https://doi.org/10.1017/aer.2020.64 Published online by Cambridge University Press

determined by the duct volume effect, i.e., a storage effect of mass and energy. The perturbations, on a fundamental level, can be classified into three types: acoustic wave, vorticity wave and entropy wave. If the flow is uniform and parallel, these perturbations are independent of each other, and their effects are linearly superimposed. When any one of these perturbations reaches the choking flow at the throttle throat, a transient is initiated that gives rise to two new acoustic waves (one in each direction) and also a vorticity and an entropy wave. These four waves will be referred to as product waves. Of these, acoustic waves are capable of propagating both upstream and downstream at the speed of sound relative to the gas. Vorticity and entropy waves are convected downstream at the flow speed. Only the upstream acoustic wave is capable of propagating into and affecting the shock wave. For the present study, the flow is thought of as a known steady flow onto which the dominant unsteady effects are superimposed. The dominant unsteady effects, from what has been discussed above, involve shock wave propagation, duct volume effect and the upstream acoustic wave propagation. In Ref. (25), we have provided a dynamic model to describe the bistability phenomena of shock motion. In this paper, we will further present a dynamic model to describe the multistability phenomena of ramjet engine, and this is its main difference from the previous one. Moreover, the new model has taken the combustion heat addition into account, which enables a thorough description of the whole dynamics of the engine, while the previous one can only describe the dynamics of shock motion in a supersonic diffuser.

2.1 Shock dynamics

The shock wave responds to both upstream and downstream perturbations. Consideration is now limited to downstream perturbations. As presented in Ref. (25), the dynamic model of shock motion can thus be obtained as

$$\frac{\dot{x}_s}{\bar{a}_1(x_s)} = -\frac{k+1}{4k\bar{M}_1(x_s)}\frac{1}{\bar{p}_1(x_s)}\left[p_2 - \bar{p}_2(x_s)\right] \qquad \ldots (1)$$

where p_2 denotes the perturbation downstream of the shock wave, x_s denotes the position of shock wave, k denotes the ratio of specific heats, and the variables $\bar{a}_1$ (speed of sound), $\bar{p}_1$ (static pressure) and $\bar{M}_1$ (Mach number) denote the corresponding steady-state parameters.

2.2 Upstream acoustic wave propagation

The downstream pressure perturbations that arise from the choking flow at the throttle throat will produce acoustic waves, which propagate upstream to the shock wave. The model of upstream acoustic wave propagation was given in Ref. (25). But in this paper, a frictionless constant-area burner has been added, compared to the physical model in Ref. (25). The effect of combustion on the amplitude variation of acoustic wave propagation must be considered.

The acoustic wave propagation involves time delay, amplitude variation and waveform variation due to the variation in wave speed with amplitude. Only the first two effects are considered. The propagation velocity is the speed of sound, which depends on the local temperature. The propagation also takes place within a variable Mach number flow. The calculation of the forward propagation time constant σ can be solved as

$$\sigma = \int_{x_{th}}^{x_s} \frac{1}{v(x) - a(x)}dx = \int_{x_{th}}^{x_s} \frac{1}{[M(x)-1]\sqrt{kRT_0\{1 + [1/2(k-1)]M(x)^2\}^{-1}}}dx \qquad \ldots (2)$$

https://doi.org/10.1017/aer.2020.64 Published online by Cambridge University Press

where

$$M(x) = q^{-1}[A_{th}/A(x)] \quad \ldots(3)$$

and

$$q(M) = M\left[\frac{2}{k+1}\left(1+\frac{k-1}{2}M^2\right)\right]^{-\frac{k+1}{2(k-1)}} \quad \ldots(4)$$

Proximately, the upstream acoustic wave propagation can be described by adopting a simple first order transient response model, which is given by

$$\frac{dp_2}{dt} = -\frac{1}{\sigma}\left[p_2 - \Omega(x_s)p_{th}\right] \quad \ldots(5)$$

where $\Omega(x_s)$ denotes the amplitude variation against the shock position, and the variation is induced by the heat addition in the combustor.

If the normal shock locates within the inlet, then

$$\Omega(x_s) = \frac{A_5/A_3}{\sqrt{\tau}\,q\left\{\Phi^{-1}\left\{\frac{\Phi\left[q_{sub}^{-1}(A_5/A_3)\right]}{\sqrt{\tau}}\right\}\right\}} \times \left(\frac{k+1}{2+(k-1)\left\{q_{sub}^{-1}\left[\frac{A_3}{A_s(x_s)}q\left\{\Phi^{-1}\left\{\frac{\Phi\left[q_{sub}^{-1}(A_5/A_3)\right]}{\sqrt{\tau}}\right\}\right\}\right]\right\}^2}\right)^{\frac{k}{k-1}} \quad \ldots(6)$$

where

$$\Phi(M) = M\left[1+\left(\frac{k-1}{2}\right)M^2\right]^{1/2} \Big/ \sqrt{1+kM^2} \quad \ldots(7)$$

and q_{sub}^{-1} is the subsonic solution of the inverse function q^{-1}.

If the normal shock locates within the combustor, then

$$\Omega(x_s) = \frac{A_5/A_3\sqrt{\tau(x_s)/\tau}}{q\left\{\Phi^{-1}\left\{\Phi\left[q_{sub}^{-1}(A_5/A_3)\right]\sqrt{\frac{\tau(x_s)}{\tau}}\right\}\right\}} \quad \ldots(8)$$

$$\times \left(\frac{k+1}{2+(k-1)\left\{\Phi^{-1}\left\{\Phi\left[q_{sub}^{-1}(A_5/A_3)\right]\sqrt{\frac{\tau(x_s)}{\tau}}\right\}\right\}^2}\right)^{\frac{k}{k-1}} \quad \ldots(8)$$

https://doi.org/10.1017/aer.2020.64 Published online by Cambridge University Press

If the normal shock locates within the nozzle, then

$$\Omega(x_s) = \left\{ \frac{k+1}{2+(k-1)\{q_{sub}^{-1}[A_5/A_s(x_s)]\}^2} \right\}^{\frac{k}{k-1}} \quad \ldots (9)$$

where $\tau(x) \equiv T_t(x)/T_{t3}$, and it is represented in non-dimensional form by a rational function (ratio of polynomial functions) given by

$$\tau(x) = 1 + (\tau - 1)\left\{ \frac{\theta\chi}{1+(\theta-1)\chi} \right\}, \quad \theta \geq 1 \quad \ldots (10)$$

where $\chi \equiv (x - x_i)/(x_4 - x_i)$, $\tau \equiv T_{t4}/T_{t3}$, x_i is the axial location at which heat addition begins, and θ is an empirical constant, which depends on the mode of fuel injection and mixture.

2.3 Duct volume effect

Volume effect is a dominant unsteady process that indicates the air in the inlet volume varies along with time in a dynamic progress, bringing the storage effect of mass and energy. The continuity equation can be described as follow

$$\dot{m}_\infty - \dot{m}_{th} = \frac{dm}{dt} \quad \ldots (11)$$

where the mass change can be expanded as follow

$$\dot{m}_\infty - \dot{m}_{th} = \frac{d(\rho_{th}\mathrm{V})}{dt} \quad \ldots (12)$$

where V is plenum volume of the duct. The density change will be related to the changes in plenum pressure by

$$\frac{d\rho_{th}}{dt} = \frac{\rho_{th}}{kp_{th}}\frac{dp_{th}}{dt} \quad \ldots (13)$$

The expression for mass conservation in the plenum can thus be written as

$$\frac{dp_{th}}{dt} = -\frac{kp_{th}}{V\rho_{th}}[\dot{m}_{th} - \dot{m}_\infty] + \frac{kp_{\mathrm{th}}A_{th}}{V}\frac{dx_s}{dt} \quad \ldots (14)$$

where

$$\dot{m}_{th} = K[1 + {}^1\!/_2(k-1)]^{k/(k-1)}A_{th}p_{th}/\sqrt{T_\infty} \quad \ldots (15)$$

$$K = \sqrt{\frac{k}{R}\left(\frac{2}{k+1}\right)^{\frac{k+1}{k-1}}} \quad \ldots (16)$$

https://doi.org/10.1017/aer.2020.64 Published online by Cambridge University Press

When the normal shock locates inside of the engine, the captured mass flow rate can be expressed as

$$\dot{m}_\infty = Kq(M_\infty)A_0 p_{t\infty}/\sqrt{T_{t\infty}} \quad \ldots(17)$$

When the inlet unstarts, the captured mass flow rate can be expressed as

$$\dot{m}_\infty = Kq(M_\infty)A_\infty(x_s)p_{t\infty}/\sqrt{T_{t\infty}} \quad \ldots(18)$$

where A_∞ is the inlet capture area.

To scale the variables in these equations to a dimensionless form, the shock position is nondimensionalised using the characteristic length l (length from "0" to "th"), the time variable using the characteristic time l/v_∞, the mass flow rate using the quantity $\rho_\infty v_\infty A_0$, and the pressure using $1/2\rho_\infty a_\infty^2$ as follows

$$\begin{cases} \tilde{x}_s = \frac{x_s}{l} \\ \tilde{t} = \dfrac{t}{l/v_\infty} \\ \tilde{p} = \dfrac{p}{1/2\rho_\infty a_\infty^2} \\ \dot{\tilde{m}} = \dfrac{\dot{m}}{\rho_\infty v_\infty A_0} \end{cases} \quad \ldots(19)$$

Definitions of these variables allow expressing models in the dimensionless representation

$$\begin{cases} \dfrac{d\tilde{x}_s}{d\tilde{t}} = -\dfrac{k+1}{4k\bar{M}_1}\dfrac{\bar{a}_1}{v_\infty}\dfrac{1}{\bar{\tilde{p}}_1}[\tilde{p}_2 - \tilde{\bar{p}}_2(\tilde{x}_s)] \\ \dfrac{d\tilde{p}_2}{d\tilde{t}} = -\dfrac{1}{\sigma v_\infty/l}[\tilde{p}_2 - \Omega(\tilde{x}_s)\tilde{p}_{th}] \\ \dfrac{d\tilde{p}_{th}}{d\tilde{t}} = -\tau\dfrac{4A_0 l}{(k+1)V}\dfrac{4kRT_\infty}{a_\infty^2}[\dot{\tilde{m}}_{th} - \dot{\tilde{m}}_\infty(\tilde{x})] + \dfrac{kA_{th}l}{V}\tilde{p}_{th}\dfrac{d\tilde{x}_s}{d\tilde{t}} \end{cases} \quad \ldots(20)$$

The coupled nonlinear are the equations that are to be solved in order to predict the transient behaviours of shock motion in the ramjet engine.

3.0 DYNAMIC SIMULATIONS OF THE COMBUSTOR-INLET INTERACTIONS IN A CLASSIFICATION FRAMEWORK

In previous studies, the combustor-inlet interactions in ramjet engines have been classified by using discrete mathematics. The studies, however, were performed in a static framework and can only make a direct, instantaneous link between system states and external perturbations using algebraic relationships. The main obstacle is that the algebraic equations cannot account for the dominant dynamic processes of the system, such as the unstable positive-feedback effect and the duct-volume effect. These effects are inherited in the system and have strong

https://doi.org/10.1017/aer.2020.64 Published online by Cambridge University Press

Table 1
Parameters for the dynamic simulations

Class	M_∞	A_m/A_0	A_3/A_0	A_{th}/A_0
Type I	1.8	0.8	1.1	0.6
Type II	2	0.9	1.1	0.8
Type III	2	0.85	0.9	0.78
Type IV	2	0.7	1.1	0.7
Type V	2	0.85	0.95	0.8
Type VI	3	0.9	0.95	0.75
Type VII	3	0.8	0.9	0.75
Type VIII	3	0.95	1.2	0.75
Type IX	3	0.95	1.1	0.8
Type X	3.5	0.9	1.4	0.9
Type XI	3	0.8	1.1	0.95

In the root level of the classification, the 11 types of combustor-inlet interactions fall into three categories: "not startable," "not restartable" and "restartable."

influence on the combustor-inlet interactions in ramjet engine. In this section, the dynamic behaviours of the combustor-inlet interactions will be simulated in a classification framework as presented in Ref. (29) where we have used the concept of classification to mathematically rationalise the complexity of combustor-inlet interactions, and proved analytically that there are mathematically 72 types of combustor-inlet interactions in a ramjet engine, 11 of which are physically existent.

Now that we have developed the low order dynamic model of the nonlinear shock motion, we will use the model to explore the transient shock motion in response to external changes under different combustor-inlet interactions. Simulations are performed under different incoming flow conditions and geometric parameters as presented in Table 1. The ordinary differential equations are numerically solved using the fourth-order Runge-Kutta method. The time scale is chosen to be 10^{-4}s, which is much less than the characteristic time scale of the dominant unsteady effects, such as upstream acoustic wave propagation and duct-volume effect. As the original point is set at the inlet entrance $\tilde{x}_0 = 0$, the other non-dimensional positions are $\tilde{x}_m = 0.16$, $\tilde{x}_3 = 0.65$, $\tilde{x}_4 = 0.87$ and $\tilde{x}_{th} = 1$, respectively. Under these conditions, the 11 types of combustor-inlet interactions can be expressed in a dynamic framework.

3.1 Not startable

This category corresponds to such situation that the inlet is not startable, generally appearing as the so-called "low Mach number unstart." It indicates that the engine cannot operate either in the ramjet mode or in the scramjet mode. Type I combustor-inlet interaction is the only one that goes with this category. Figure 3 shows the dynamic response of shock position to time following step decrease in the total hear addition rate τ from a value to one (no heat addition). The curve P_{UU} shows that the detached shock wave moves asymptotically toward the inlet entrance, but cannot be swallowed into the inlet even when no heat is added into the combustor. In the transient process, the decrease of heat addition increases the flow capacity of the nozzle, resulting in the imbalance in the mass flow rate. The plenum pressure will then change slightly due to the duct volume effect; this perturbation propagates upstream

https://doi.org/10.1017/aer.2020.64 Published online by Cambridge University Press

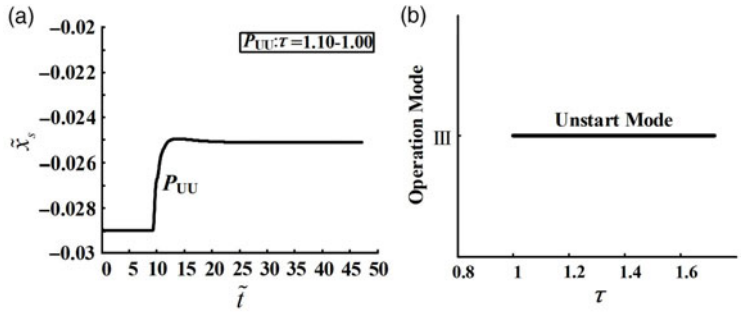

Figure 3. Dynamic simulations of type I combustor-inlet interaction. $M_\infty = 1.8, A_m/A_0 = 0.8, A_3/A_0 = 1.1, A_{th}/A_0 = 0.6$. a) Transient process, b) Type I combustor-inlet interaction

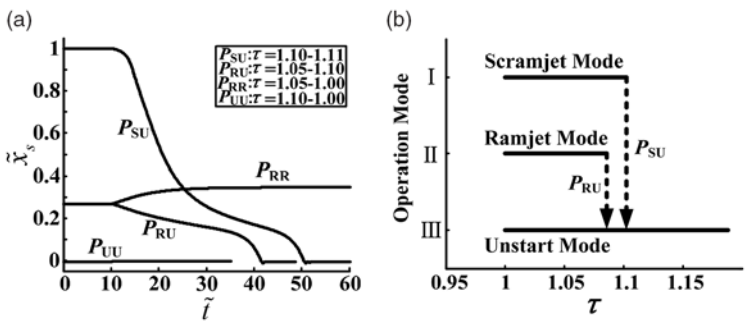

Figure 4. Dynamic simulations of type II combustor-inlet interaction. $M_\infty = 2, A_m/A_0 = 0.9, A_3/A_0 = 1.1, A_{th}/A_0 = 0.8$. a) Transient process, b) Type II combustor-inlet interaction

by acoustic wave propagation to influence the dynamics of shock wave, and as a result the shock wave moves asymptotically toward another equilibrium state. In the case, the engine has limited flow capture capacity. Thus there is always a detached shock to provide overflow to match the flow balance.

3.2 Not restartable

Within the 11 types of combustor-inlet interactions, 4 types as shown in Figs. 4–7 can be grouped into this category. The similarity each type shares is that the inlet is not restartable. That is, the flight Mach number is high enough to start the inlet, but the engine fails to restart the inlet once inlet unstarts. The transient processes are shown by the curve P_{UU} in Figs. 4–7. When the inlet is unstart, the decrease of heat addition ratio τ will increase the mass flow rate at the throttle throat. In response, the detached shock moves asymptotically back to the inlet entrance to reduce overflow. But the detached shock cannot reach the entrance of the inlet and can only be located ahead of the inlet entrance.

Generally, when the engine operates in the scramjet mode, the increase of the heat addition rate to a critical value will result in the flow choking at the nozzle throat. The choking mechanism in supersonic flow gives rise to the appearance of shock wave at the nozzle throat. Under the critical condition, the flow Mach number upstream of the shock is one, and then a slight increase of the heat addition will cause the shock wave move upstream. The shock wave will leave the convergent channel of the nozzle quickly because of the existence of instability

https://doi.org/10.1017/aer.2020.64 Published online by Cambridge University Press

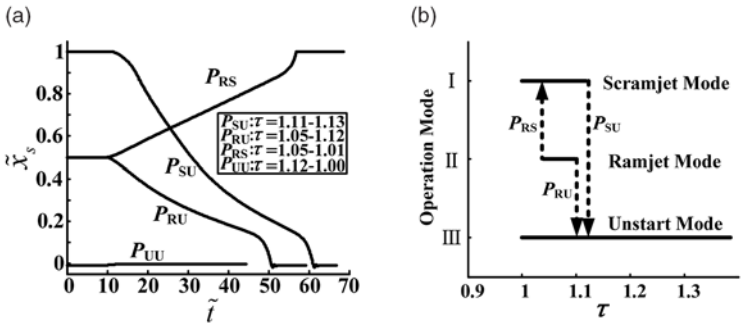

Figure 5. Dynamic simulations of type III combustor-inlet interaction. $M_\infty = 2, A_m/A_0 = 0.85, A_3/A_0 = 0.9, A_{th}/A_0 = 0.78$. a) Transient process, b) Type III combustor-inlet interaction

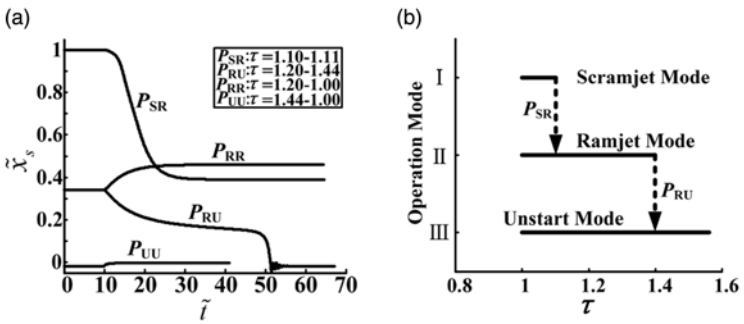

Figure 6. Dynamic simulations of type IV combustor-inlet interaction. $M_\infty = 2, A_m/A_0 = 0.7, A_3/A_0 = 1.1, A_{th}/A_0 = 0.7$. a) Transient process, b) Type IV combustor-inlet interaction

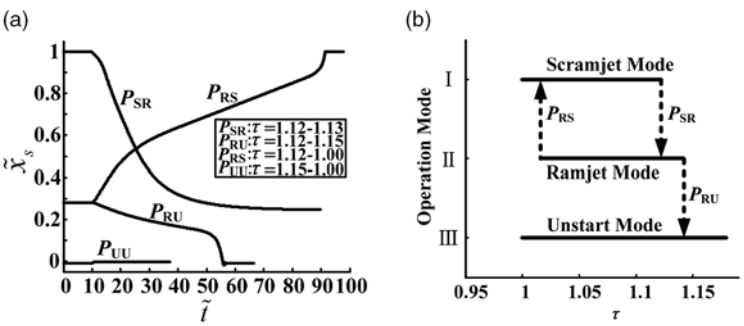

Figure 7. Dynamic simulations of type V combustor-inlet interaction. $M_\infty = 2, A_m/A_0 = 0.85, A_3/A_0 = 0.95, A_{th}/A_0 = 0.8$. a) Transient process, b) Type V combustor-inlet interaction

mechanism, and move upstream into the diverging channel of the inlet. At this time, the total pressure recovery at the nozzle throat, as well as the flow capacity, will increase when the shock approaches the inlet throat. When the shock wave reaches the inlet throat, but the flow capacity at the nozzle throat is still not high enough to balance the incoming flow mass rate, the shock wave will continue to move upstream and the inlet unstarts. The transient processes are shown by the curve P_{SU} in Figs. 4 and 5. Otherwise, the shock wave can be stabilised in

https://doi.org/10.1017/aer.2020.64 Published online by Cambridge University Press

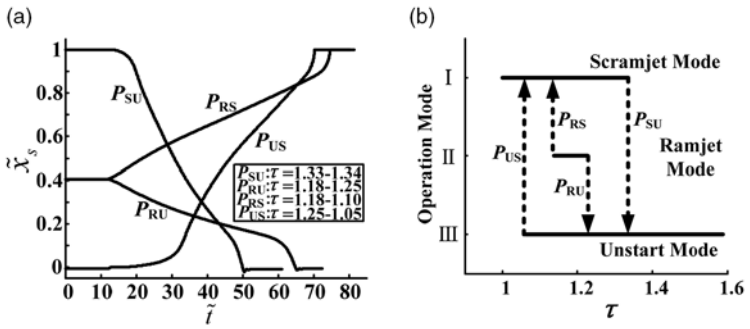

Figure 8. Dynamic simulations of type VI combustor-inlet interaction. $M_\infty = 3, A_m/A_0 = 0.9, A_3/A_0 = 0.95, A_{th}/A_0 = 0.75$. a) Transient process, b) Type VI combustor-inlet interaction

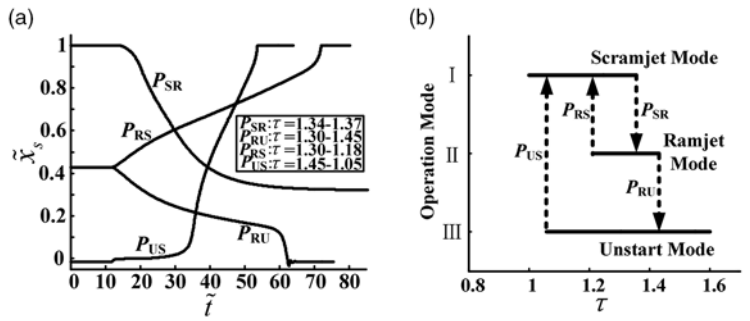

Figure 9. Dynamic simulations of type VII combustor-inlet interaction. $M_\infty = 3, A_m/A_0 = 0.8, A_3/A_0 = 0.95, A_{th}/A_0 = 0.75$. a) Transient process, b) Type VII combustor-inlet interaction

the divergent channel of the inlet, and the transient processes are shown by the curve P_{SR} in Figs. 6 and 7.

Generally, when the engine initially operates in the ramjet mode, the decrease of the heat addition rate will increase the flow capacity of the nozzle throat. The plenum pressure will then decrease dynamically to balance the mass flow rate of the engine; this perturbation propagates upstream by acoustic wave propagation to influence the dynamics of shock wave, and as a result the shock wave moves asymptotically toward the exit of the inlet. For one case, further decrease of the heat addition will cause the shock wave to move toward the nozzle throat and finally disappear. For the other, even the heat release is decreased to zero; the shock wave can only be stabilised in the divergent channel of the inlet. The transient processes of the formal case are shown by the curve P_{RS} in Figs. 5 and 7. The transient processes of the latter case are shown by the curve P_{RR} in Figs. 4 and 6.

3.3 Restartable

The last six types of combustor-inlet interactions as shown in Figs. 8–13 can be grouped into this category. The similarity each type shares is that the inlet is restartable. It indicates that the engine has high flow capacity. Once the inlet unstarts, it can be restarted simply by decreasing the heat addition.

https://doi.org/10.1017/aer.2020.64 Published online by Cambridge University Press

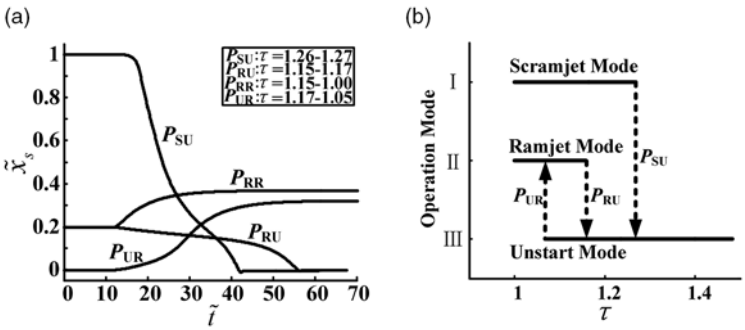

Figure 10. Dynamic simulations of type VIII combustor-inlet interaction. $M_\infty = 3, A_m/A_0 = 0.95, A_3/A_0 = 1.2, A_{th}/A_0 = 0.75$. a) Transient process, b) Type VIII combustor-inlet interaction

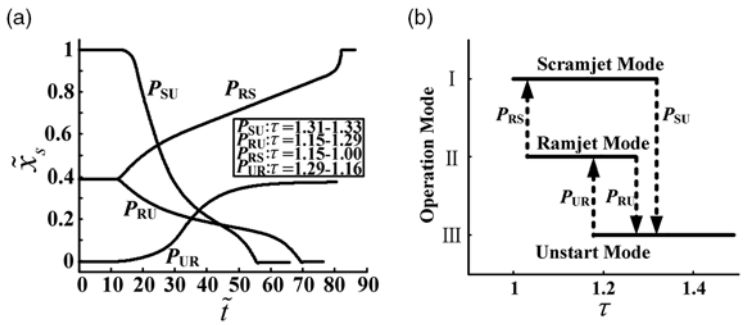

Figure 11. Dynamic simulations of type IX combustor-inlet interaction. $M_\infty = 3, A_m/A_0 = 0.95, A_3/A_0 = 1.1, A_{th}/A_0 = 0.8$. a) Transient process, b) Type IX combustor-inlet interaction

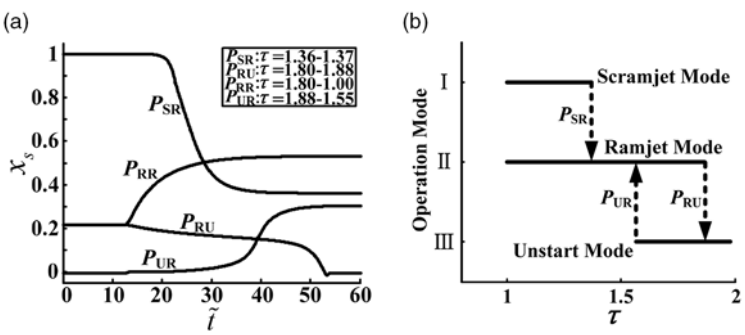

Figure 12. Dynamic simulations of type X combustor-inlet interaction. $M_\infty = 3.5, A_m/A_0 = 0.9, A_3/A_0 = 1.4, A_{th}/A_0 = 0.9$. a) Transient process, b) Type X combustor-inlet interaction

When the engine initially operates in the unstarted state, the decrease of heat addition increases the flow capacity of the nozzle. The plenum pressure will then change slightly and this perturbation will propagate upstream by acoustic wave propagation to influence the dynamics of shock wave, and the shock wave moves asymptotically toward the entrance of the inlet. In the case, the engine has enough flow capture capacity, and under critical conditions

https://doi.org/10.1017/aer.2020.64 Published online by Cambridge University Press

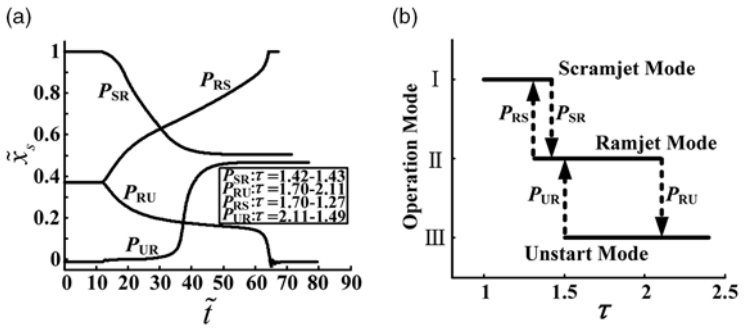

Figure 13. Dynamic simulations of type XI combustor-inlet interaction. $M_\infty = 3, A_m/A_0 = 0.8, A_3/A_0 = 1.1, A_{th}/A_0 = 0.95$. a) Transient process, b) Type XI combustor-inlet interaction

the shock wave can move to the entrance of the inlet. At this moment, even a slight decrease of the heat addition will cause the shock wave move into the inlet and leave the convergent channel of the inlet at a high speed. Subsequently, if the choking conditions of the nozzle throat flow are no longer satisfied, the shock wave will move towards the nozzle throat and finally disappear. As a result the engine operates in the scramjet mode. Otherwise the shock wave will be stabilised at a position of the divergent channel of the inlet, and the engine operates in the ramjet mode. The transient processes of the formal case are shown by the curve P_{US} in Figs. 8 and 9. The transient processes of the latter case are shown by the curve P_{UR} in Figs. 10–13. When the engine initially operates in the ramjet mode, the increase of the heat addition will cause the shock wave move upstream, and the inlet will finally unstart if the total heat addition is high enough. The transient processes the mode transitions are shown by the curve P_{RU} in Figs. 8–13. On the contrary, the decrease of the heat addition will cause the shock wave to move downstream. Subsequently there will be two cases that happen when further decreasing the heat addition, as shown by the curve P_{RS} in Figs. 8, 9, 11 and 13, or by the curve P_{RR} in Figs. 10 and 12.

4.0 CONCLUSIONS

A dynamic model is developed analytically to capture the complex combustor-inlet interactions in a ramjet engine. This model, consisting of a set of nonlinear, first-order differential equations, allows for rapid calculations of system's dynamics and can be a starting point toward a control-oriented dynamic model of ramjet engines. At present, the model can describe the multiple stable states of the engine and the corresponding nonlinear effects such as irreversibility, coexistence, hysteresis and various mode transitions in a dynamic framework. In contrast to the previous static analysis, the advantage of this dynamical model is the capability to simulate and analyse the dynamics behaviour of the engine not only in the steady state but also in the transient regime. Specially, its distict character lies in the capability of describing the unstable processes in the transitions between the multiple stable states of the engine, and thereby it reveals that the corresponding unstable mechanisms have significant influence on the whole engine's nonlinear interactions. On the base of the model's capability in describing the unstable mechanisms of the engine, we extend the previous studies of the classification of combustor-inlet interactions from a static framework to a dynamic framework, which helps to clarifying the transient processes of the various combustor-inlet

https://doi.org/10.1017/aer.2020.64 Published online by Cambridge University Press

interactions, and further advancing our understanding of the nonlinear phenomena induced by these nonlinear interactions.

ACKNOWLEDGMENTS

Financial supports from the National Natural Science Foundation of China (Grant No. 51976182) are gratefully acknowledged.

REFERENCES

1. ZHA, G.C., KNIGHT, D., SMITH, D. and HAAS, M. Numerical simulation of high-speed civil transport inlet operability with angle of attack, *AIAA J.*, 1998, **36**, (7), pp 1223–1229.
2. CHOI, J.Y., JEUNG, I.S. and YOON, Y. Numerical study of scram accelerator starting characteristics, *AIAA J.*, 1998, **36**, (6), pp 1029–1038.
3. OGAWA, H. and BOYCE, R.R. Physical insight into scramjet inlet behavior via multi-objective design optimization, *AIAA J.*, 2012, **50**, (8), pp 1773–1783.
4. HUANG, W., YAN, L. and TAN, J.G. Survey on the mode transition technique in combined cycle propulsion systems, *Aerosp. Sci. Technol.*, 2014, **39**, pp 685–691.
5. SULLINS, G.A. Demonstration of mode transition in a scramjet combustor, *J. Propuls. Power*, 1993, **9**, (4), pp 515–520.
6. CHUN, J., SCHEUERMANN, T., VON WOLFERSDORF, J. and WEIGAND, B. Experimental Study on Combustion Mode Transition in a Scramjet with Parallel Injection, AIAA 2006-8063, 2006.
7. EGGERS, T., NOVELLI, P. and HAUPT, M. Design Studies of the JAPHAR Experimental Vehicle for Dual Mode Ramjet Demonstration, AIAA 2001-1921, 2001.
8. GOYNE, C.P., MCDANIEL, J.C., QUAGLIAROLI, T.M., KRAUSS, R.H. and DAY, S.W. Dual-mode combustion of hydrogen in a mach 5, continuous-flow facility, *J. Propuls. Power*, 2001, **17**, (6), pp 1313–1318.
9. RIGGINS, D., TACKETT, R., TAYLOR, T. and AUSLENDER, A. Thermodynamic Analysis of Dual-Mode Scramjet Engine Operation and Performance, AIAA 2006-8059, 2006.
10. LAURENCE, S.J., KARL, S., MARTINEZ SCHRAMM, J. and HANNEMANN, K. Transient fluid-combustion phenomena in a model scramjet, *J. Fluid Mech.*, 2013, **722**, pp 85–120.
11. FERRI, A. Review of problems in application of supersonic combustion, *J. R. Aeronaut. Soc.*, 1964, **68**, (645), pp 575–597.
12. BILLIG, F.S. and DUGGER, G.L., The interaction of shock waves and heat addition in the design of supersonic combustors, *Symp. Combust.*, 1969, **12**, (1), pp 1125–1139.
13. CURRAN, E. Fluid phenomena in scramjet combustion systems, *Annu. Rev. Fluid Mech.*, 1996, **28**, (1), pp 323–360.
14. SHIMURA, T., MITANI, T., SAKURANAKA, N. and IZUMIKAWA, M. Load oscillations caused by unstart of hypersonic wind tunnels and engines, *J. Propuls. Power.*, 1998, **14**, (3), pp 348–353.
15. S. O'BYRNEYRNE, DOOLAN, M., OLSEN, S.R. and HOUWING, A.F.P. Analysis of transient thermal choking processes in a model scramjet engine, *J. Propuls. Power.*, 2000, **16**, (5), pp 808–814.
16. KOBAYASHI, K., KANDA, T., TOMIOKA, S., TANI, K., SAKURANAKA, N. and MITANI, T. Suppression of combustor-inlet interaction in a scramjet engine under mach 4 flight conditions, *Trans. Jpn. Soc. Aeronaut. Space Sci.*, 2007, **49**, (166), pp 246–253.
17. SANTANA, E.R. and WEIGAND, B. Numerical Investigations of Inlet-Combustor Interactions for a Scramjet Hydrogen-fueled engine at a Mach Flight Number of 8, AIAA 2012-5926, 2012.
18. GAMBA, M., MILLER, V., MUNGAL, G. and HANSON, R. Combustion characteristics of an inlet/supersonic combustor model, AIAA 2012-0612, 2012.
19. CHEN, C.P., SAJBEN, M. and KROUTIL, J.C. Shock-wave oscillations in a transonic diffuser flow, *AIAA J.*, 1979, **17**, (10), pp 1076–1083.
20. BOGAR, T.J., SAJBEN, M. and KROUTIL, J.C. Characteristic frequencies of transonic diffuser flow oscillations, *AIAA J.*, 1983, **21**, (9), pp 1232–1240.
21. SAJBEN, M., BOGAR, T.J. and KROUTIL, J.C. Forced oscillation experiments in supercritical diffuser flows, *AIAA J.*, 1984, **22**, (4), pp 465–474.

22. BOGAR, T.J., SAJBEN, M. and KROUTIL, J.C. Response of a supersonic inlet to downstream perturbations, *J. Propuls. Power.*, 1985, **1**, (2), pp 118–125.
23. SAJBEN, M., BOGAR, T.J. and KROUTIL, J.C., Experimental study of flows in a two-dimensional inlet model, *J. Propuls. Power.*, 1985, **1**, (2), pp 109–117.
24. VAN WIE, D.M., KWOK, F.T. and WALSH, R.F. Starting Characteristics of Supersonic Inlets, AIAA 1996-2914, 1996.
25. CUI, T., WANG, Y. and YU, D.R. Bistability and hysteresis in a nonlinear dynamic model of shock motion, *J. Aircr.*, 2014, **51**, (5), pp 1373–1379.
26. CULICK, F.E.C. and ROGERS, T. The response of normal shocks in diffusers, *AIAA J.*, 1983, **21**, (10), pp 1382–1390.
27. HSIEH, S.Y. and YANG, V. A unified analysis of unsteady flow structures in a supersonic ramjet engine, AIAA 1997-0396, 1997.
28. CUI, T. and TANG, S. Geometry rule of combustor–inlet interaction in Ramjet engines, *J. Propuls. Power.*, 2014, **30**, (2), pp 449–460.
29. CUI, T., WANG, Y., LIU, K. and JIN, J. Classification of combustor–inlet interactions for airbreathing Ramjet propulsion, *AIAA J.*, 2015, **53**, (8), pp 2237–2255.
30. MACMARTIN, D.G. Dynamics and control of shock motion in a near-isentropic inlet, *J. Aircr.*, 2004, **41**, (4), pp 846–853.
31. PARK, J.W., PARK, I.S., SEO, B.G., SUNG, H.G., ANANTHKRISHINAN, N. and TAHK, M.J. Optimal terminal shock position under disturbances for ramjet supercritical operation, *J. Propuls. Power.*, 2012, **29**, (1), pp 238–248.
32. PARK, I.S., KIM, S.K., YEOM, H.W., SUNG, H.G., PARK, J.W. and TAHK, M.J. Control-oriented model for intake shock position dynamics in ramjet engine, *J. Propuls. Power.*, 2011, **27**, (2), pp 499–502.
33. TOURNES, C., LANDRUM, D.B., SHTESSEL, Y. and HAWK, C.W. Ramjet-powered reusable launch vehicle control by sliding modes, *J. Guid. Control. Dyn.*, 1998, **21**, (3), pp 409–415.
34. CHANDRA, K.P.B., GUPTA, N.K., ANANTHKRISHNAN, N., PARK, I.S. and YOON, H.G. Modeling, simulation, and controller design for an air-breathing combustion system, *J. Propuls. Power.*, 2010, **26**, (3), pp 562–574.

https://doi.org/10.1017/aer.2020.64 Published online by Cambridge University Press